

First Constraints on Compact Dark Matter from Fast Radio Burst Microstructure

MAWSON W. SAMMONS,¹ JEAN-PIERRE MACQUART,² RON D. ETERS,^{3,2} RYAN M. SHANNON,⁴ HYERIN CHO,⁵
J. XAVIER PROCHASKA,⁶ ADAM T. DELLER,⁴ AND CHERIE K. DAY^{4,3}

¹*Curtin University, Perth, WA 6845, Australia*

²*International Centre for Radio Astronomy Research, Curtin Institute of Radio Astronomy, Curtin University, Perth, WA 6845, Australia*

³*CSIRO Astronomy and Space Science, PO Box 76, Epping, NSW 1710, Australia*

⁴*Centre for Astrophysics and Supercomputing, Swinburne University of Technology, Hawthorn VIC 3122, Australia*

⁵*School of Physics and Chemistry, Gwangju Institute of Science and Technology, Gwangju, 61005, Korea*

⁶*University of California, Santa Cruz, 1156 High St., Santa Cruz, CA 95064, USA*

(Received December 21, 2024; Revised December 21, 2024; Accepted December 21, 2024)

Submitted to ApJ

ABSTRACT

Despite existing constraints it remains possible that up to 35% of all dark matter is comprised of compact objects, such as the black holes in the 10-100 M_{\odot} range whose existence has been confirmed by LIGO. The strong gravitational lensing of transients such as FRBs and GRBs has been suggested as a more sensitive probe for compact dark matter than intensity fluctuations observed in microlensing experiments. Recently ASKAP has reported burst substructure down to $15\mu\text{s}$ timescales in FRBs in the redshift range $0.3 - 0.5$. We investigate here the implications of this for the detectability of dark matter by FRBs. A sample size of $\sim 10^3$ localized FRBs is required to exclude the fraction of dark matter in compact objects in the 10-100 M_{\odot} range, residing in intercepted individual galaxy halos (with impact distances $\lesssim 50$ kpc) along FRB sightlines, to less than 35% with 95% confidence. Approximately 10^2 localised FRBs would be required to constrain dark matter to a similar level if it were distributed along $\gtrsim 1$ Gpc-long FRB sightlines through the cosmic web. Conversely, existing constraints on the fraction of compact dark matter permit as many as 1 in ≈ 50 of all $z \lesssim 0.4$ FRBs to exhibit micro-lensed burst structure. We further consider the constraints that recently observed high time resolution FRB pulse profiles place on dark matter substructure on yet smaller scales, through the cumulative effect of a large collection of tiny lenses on the pulse profile; we conclude that, even if present, their effect is likely not yet observed.

Keywords: Gravitational lensing (670), Radio transient sources (2008), Dark matter (353)

1. INTRODUCTION

Dark matter comprises 24% of the energy density of the Universe (Bennett et al. 2013), yet its indeterminate form represents one of the largest unsolved problems in astrophysics. Exotic particles from outside the standard model, such as Weakly Interacting Massive Particles (WIMPs) or axions have been invoked as possible explanations (see Bertone et al. (2005) for a review). However, some fraction of dark matter could reside in the Universe as compact objects, such as black holes or neutron stars.

Decades of extensive research has constrained the fraction of dark matter present in compact objects over a range of masses. Low mass objects ($\lesssim 10M_{\odot}$) are excluded as the dominant form of dark matter in the Milky Way and environs based on the absence of stellar variability caused by gravitational microlensing (Tisserand et al. 2007; Wyrzykowski et al. 2011; Alcock et al. 1997). High mass objects ($\gtrsim 100M_{\odot}$) are excluded by the lack of expected kinematic perturbations to wide binary orbits and ultra faint dwarf galaxies (Quinn et al. 2009; Brandt 2016).

The only population of compact objects that are not well constrained lie in the range of 10 to 100 M_{\odot} . There is a known population of black holes in this mass range; gravitational wave observations by LIGO have detected several mergers of these black holes (LIGO Scientific Collaboration and Virgo Collaboration et al. 2019). Subsequent theories suggest that dark matter composed of $\sim 30M_{\odot}$ primordial black holes could explain the merger event rates observed by LIGO (Bird et al. 2016; Clesse & Garca-Bellido 2017; Sasaki et al. 2016). Better constraints on the fraction of compact dark matter within the 10-100 M_{\odot} range could therefore be key in identifying some fraction of dark matter.

The strong gravitational lensing of extragalactic transients provides a way to either detect or to place more stringent constraints on dark matter. The strong lensing of type Ia supernovae has been used to limit the compact dark matter fraction to less than 35% for all objects more massive than 0.01 M_{\odot} (Zumalacarregui & Seljak 2018). Recently, it has been realised that cosmological transients such as Gamma Ray Bursts (GRBs) and Fast Radio Bursts (FRBs) will allow constraints to be placed at a much higher significance (Ji et al. 2018; Laha 2018).

In both cases strong lensing creates multiple images of the source. Unlike the gravitational lensing of quasars by foreground galaxies (Wong et al. 2019), the images formed by a compact object would be too close to be spatially resolved. However, the images of the source will arrive separated in time due to different gravitational and geometric time delays along each path. This temporal separation (Δt) is linearly dependent upon the lens mass, whereas the magnification ratio is mass independent. The lens mass and geometry can be constrained using these two observables. Due to the achromatic nature of gravitational lensing the same formalism initially suggested by Muoz et al. (2016) for FRBs can be applied at all wavelengths. The formalism ignores the effect of physical optics, which becomes important when the Einstein radius of the lens is smaller than the Fresnel scale, $\sim \sqrt{D_{\text{eff}}\lambda/2\pi}$, where D_{eff} is the effective distance to the lens. This occurs for lens masses less than $\sim 10^{-5}M_{\odot}$ at a frequency of 1 GHz, and is well below the masses considered here; hence a full wave optics treatment, such as that explored by Jow et al. (2020), is not yet warranted.

Several thousands of GRBs have been discovered at redshifts $z \sim 1$ by dedicated GRB observatories such as *Swift*, *BATSE*, and *Fermi*. The cosmological distances they traverse allow them to probe a large volume of the Universe for compact dark matter. GRBs have a broad temporal profile ranging from milliseconds to minutes (Ji et al. 2018), and as a result, distinguishing multiple images is more difficult as the time delay between signals lensed by a 10 M_{\odot} compact object will be less than the duration of the GRB. Ji et al. (2018) have proposed auto-correlating the light curve as a method of detecting lensing. They conclude, however, that current GRB observatories would need to reduce their noise power by at least an order of magnitude to be able to detect lensing in the 10-100 M_{\odot} mass range.

In contrast, FRBs have temporal profiles ranging from tens of microseconds (Cho et al. 2020) to several milliseconds, which is often shorter than the anticipated delay ($\sim 1\text{ms}$) for lensing by compact objects in the mass range under consideration here. This enables multiple images to be clearly distinguished, hence rendering FRBs considerably cleaner probes of compact structure along their sightlines. FRBs are highly luminous, extragalactic radio pulses, and those such as FRB 181112 (Cho et al. 2020) with substructure on timescales of a few tens of microseconds provide, to date, the finest timescale probe of sightlines at cosmological distances. Moreover, a unique capability of radio interferometric observations of such bursts is their ability to directly capture the *wavefield* of the each FRB at extremely high time resolution (3 ns; see Cho et al. 2020). This affords a powerful new diagnostic of the presence of gravitational lensing. The wavefield, which is directly observable at radio wavelengths, of any pair of lensed signals should be correlated, whereas burst substructure intrinsic to the FRB would not.

Of the FRBs localised to host galaxies so far, all have been at redshifts $z < 1$, placing the current sample generally closer in the Universe than GRBs (Ji et al. 2018; Coward et al. 2013; Bannister et al. 2019; Prochaska et al. 2019). However, this limitation is likely to be overcome with the localization of a larger sample of bursts; the existence of non-localized FRBs with dispersion measures exceeding 2000 pc cm^{-3} (e.g. Bhandari et al. 2018) ostensibly places some fraction of the population at $z > 2$.

To detect strong lensing, the temporal separation must be sufficiently large to allow each image to be distinguished. This is constrained by the shortest distinct temporal structure in the signal. In this paper we examine the implications of the high-time resolution structure observed in the localized FRBs 180924 and 181112. In FRB 180924 the shortest timescale corresponds to its rise time of only 30 μs (Farah 2020). FRB 181112 has recognisable temporal structure on the scale of 15 μs , the shortest structure observed in an extragalactic radio signal (Cho et al. 2020). The resolution of temporal structures of $\sim 10\mu\text{s}$ enables searches for lensing at temporal separations an order of magnitude below those considered in previous treatments (0.1 ms; Muoz et al. 2016; Laha 2018). Additionally, if the FRB passes close to an intervening galaxy, as it did for FRB 181112 (Prochaska et al. 2019), it opens up the possibility of examining lensing attributable to a specific galaxy along the burst sightline, other than the host galaxy or the Milky Way. Muoz et al.

(2016) and Laha (2018) report that a sample of 10^4 FRBs would be required to exclude the compact dark matter fraction to less than 1%. Assuming a Λ CDM cosmology, we apply the same formalism to estimate the constraining potential of detected high time resolution FRBs comparable to FRBs 181112 and 180924.

2. THEORY

In the weak field limit, where the gravitational potential $|\Phi| \ll c^2$, gravitational lensing can be modelled as an achromatic deflection of incident light by a thin screen. Under this treatment, a point mass lens will produce two images on the lens plane. The temporal separation, magnification ratio and position of these images are determined by the angular impact parameter of the source (β) normalised by the characteristic Einstein radius of the lens ($y = \beta/\theta_E$).

Here we briefly review previous theory as expounded by Muoz et al. (2016) and Laha (2018). Following this formalism, the difference in arrival time between the images (Δt) and the ratio of each magnification (R_f) correspond to unique normalised angular impact parameters of the source $y_{\Delta t}$ and y_{R_f} , respectively. The relation between y_{R_f} and R_f can be expressed analytically as (Laha 2018),

$$y_{R_f} = \sqrt{\frac{R_f + 1}{\sqrt{R_f}}} - 2, \quad (1)$$

which is notably independent of the lens mass. Conversely, $y_{\Delta t}$ cannot be derived analytically and is found numerically from Laha (2018):

$$\Delta t = \frac{4GM_L}{c^3}(1+z_L) \left[\frac{y}{2} \sqrt{y^2 + 4} + \ln \left(\frac{\sqrt{y^2 + 4} + y}{\sqrt{y^2 + 4} - y} \right) \right], \quad (2)$$

where M_L and z_L are the mass and redshift of the lens, respectively.

To detect gravitational lensing, we require the normalised angular impact parameter to be within the observable range (y_{\min} – y_{\max}). This range is defined by two conditions: (1) The associated time delay calculated from eq. (2) must be less than the maximum observable time delay Δt_{\max} and greater than the minimum distinguishable separation Δt_{\min} . The length of the observation sets Δt_{\max} , and Δt_{\min} is set by the structure in the pulse profile (Laha 2018). (2) The magnification ratio must be below the maximum (R_f) set by the detection threshold (Laha 2018).

For the thin screen approximation to be valid, the gravitational field at the impact parameter must also satisfy the weak field condition:

$$y_{\min} \gg \frac{R_S}{D_L \theta_E} \quad (3)$$

where R_S and D_L are respectively, the Schwarzschild radius and angular diameter distance of the lens. y_{\min} and y_{\max} define the annulus of the cross section to observable lensing. This cross section can then be used to calculate the observable lensing optical depth. Details on this calculation are provided in the following subsections for different environments. If the fraction of all dark matter that is compact (f_{DM}) is assumed to be constant, the probability of observing lensing (P_L) at least once in a set of N FRBs can then be calculated as

$$P_L = 1 - \exp \left[- \sum_i^N \tau_i \right]. \quad (4)$$

where τ_i is the optical depth of the i th FRB in the set. To exclude compact dark matter fractions of $\geq f_{\text{DM}}$ with 95% confidence, we require a null observation of lensing in a set of FRBs with a cumulative observable lensing optical depth of 3.0.

2.1. Lensing in galaxy halos

If we assume that compact dark matter takes the form of MACHOs (MASSive Compact Halo Objects), the only contribution to the lensing optical depth will come from the intervening galactic halos. In the local potential of a galaxy, the Hubble flow can be ignored and the optical depth calculated simply as

$$\begin{aligned} \tau &= \ell n_{\text{halo}} \sigma \\ &= \frac{16\pi^2 G \ell f_{\text{DM}} M_{\text{halo}} R_{\text{halo}}^3}{3c^2} \frac{D_L D_{LS}}{D_S} [y_{\max}^2 - y_{\min}^2] \end{aligned} \quad (5)$$

Table 1. Observational parameters for localised high time resolution FRBs

FRB	$\Delta t_{\min}(\text{s})$	$\Delta t_{\max}(\text{s})$	\bar{R}_f	Source Redshift
181112 ^a	15×10^{-6}	1.369	73.3	0.47550
180924	30×10^{-6}	1.445	64.7	0.3214

^aIntercepted a foreground galaxy at $z=0.3674$

where ℓ is the FRB path length through a galaxy halo of mass M_{halo} and radius R_{halo} ; D_L , D_{LS} , and D_S are the angular diameter distances from the observer to the lens, from the lens to the source and from the observer to the source respectively; σ is the observable lensing cross section, as described by Laha (2018); and n_{halo} is the average number density of the compact objects in the halo. For simplicity we assume a top-hat dark matter distribution and leave a more exhaustive treatment of the halo profile to a future work.

2.2. Lensing in the Intergalactic Medium

Stellar remnants unbound from their host galaxies via natal kicks or gravitational interactions present a possible source of lensing in the intergalactic medium (IGM) (Atri et al. 2019). Here, the effects of the Hubble flow cannot be ignored. As derived in Muoz et al. (2016) and Laha (2018), the optical depth to lensing of a single source by a single compact object in the IGM is

$$\begin{aligned} \tau &= \int_0^{z_s} d\chi(z_L)(1+z_L)^2 n_{\text{IGM}} \sigma \\ &= \frac{3}{2} f_{\text{DM}} \Omega_c \int_0^{z_s} dz_L \frac{H_0^2}{cH(z_L)} \frac{D_L D_{LS}}{D_S} (1+z_L)^2 [y_{\max}^2 - y_{\min}^2], \end{aligned} \quad (6)$$

where χ is the co-moving distance, n_{IGM} is the average co-moving number density of the lens, $H(z_L)$ is Hubble's constant at the lens redshift and Ω_c is the current density of dark matter.

Both the halo and IGM lensing optical depths are separated into magnification and time delay-limited domains over which y_{\max} is limited by the corresponding condition. At low masses, y_{\min} increases until $y_{\min} = y_{\max}$, and the optical depth to lensing becomes zero. The halo and IGM lensing optical depths are mass independent over a large range of lens masses. This can be understood by considering equations (5) and (6), respectively. The product of the Einstein radius squared and the projected number density is mass independent. Hence, by expressing the cross section in terms of the normalised angular impact parameters y_{\min} and y_{\max} , the source of the mass dependence in each optical depth becomes isolated to y_{\min} and y_{\max} . In the magnification-limited domain, y_{\max} is given by y_{R_f} and will be independent of the mass (eq. 1). If y_{\max} is also much greater than y_{\min} , then the optical depth to observable lensing in either the halo or IGM case will be effectively mass independent. The domain of this mass independent regime is determined by the minimum and maximum temporal separations.

3. RESULTS

The determination of the redshift of an FRB allows the formalism outlined in Section 2 to be applied. Here, we calculate the halo and IGM lensing optical depth for localised FRBs 181112 (Prochaska et al. 2019) and 180924 (Bannister et al. 2019). The temporal microstructure of these bursts has been resolved, enabling us to probe to the minimum value of y_{\min} allowed by the burst structure. FRBs 181112 and 180924 probe a similar range of masses ($0.1M_{\odot} \lesssim M \lesssim 10^4 M_{\odot}$) due to their similar minimum and maximum temporal separations (Table 1). Over this range of masses, eq. (3) is satisfied, and the strong field region is orders of magnitude smaller than the spatial scale probed by a temporal separation of $10 \mu\text{s}$. This is the scale of the smallest distinguishable temporal separation amongst known FRBs; therefore, the weak field approximation is valid for all cases considered here.

The spectra of FRB 181112 shown in Fig. 1 (see also Cho et al. 2020) exhibits multi-peaked structure that could potentially be explained by gravitational lensing. Indeed, if the two major peaks are assumed to be two images, the temporal profile is consistent with gravitational lensing by a $\sim 10M_{\odot}$ compact object in the halo of the foreground galaxy. Cho et al. (2020) test for the presence of microlensing by searching for correlations in the burst wavefield with

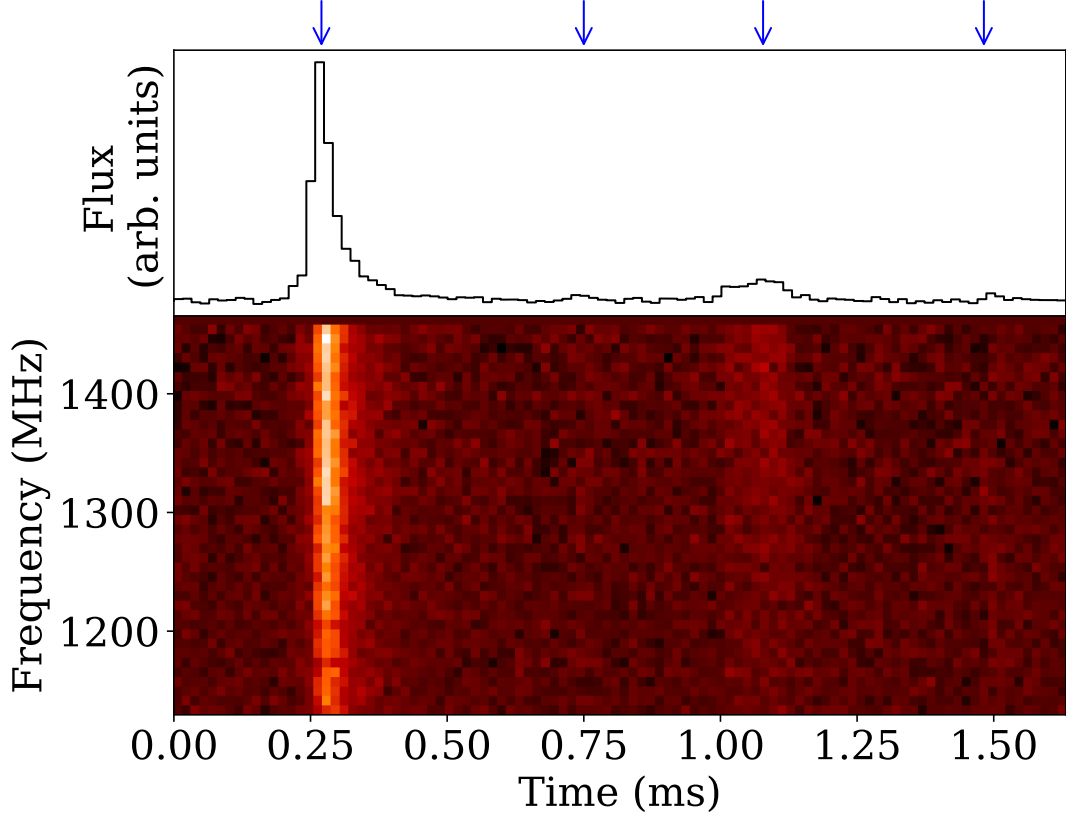


Figure 1. The pulse profile (top) and dynamic spectrum (bottom) of FRB 181112 at $16\mu\text{s}$ and 8MHz temporal and spectral resolution respectively, showing the pulse to consist of two bright sub-pulses, at $t = 0.25\text{ms}$ and 1.1ms , and two weaker sub-pulses at $t = 0.75\text{ms}$ and 1.50ms , as indicated by the blue arrows.

time; in the case of FRB 181112 no fringes between sub-pulses were seen, suggesting the pulse multiplicity is more likely intrinsic to the burst, rather than multiple lensed copies of the same burst. However, the absence of a correlation is not definitive since other effects, notably due to differences in any turbulent cold plasma encountered along the slightly separated sightlines of the lensed images, could in principle scatter the radiation in different manners, and thus destroy the phase coherence between the lensed signals. However, in the present instance [Cho et al. \(2020\)](#) also find that the detailed polarization properties of the sub-bursts differ in detail, particularly in their circular polarization, an effect which is difficult to attribute to lensing¹.

As recorded in Table 1, FRB 181112 had an extremely narrow pulse profile, with its shortest temporal structure being $15\mu\text{s}$. FRB 180924 had an extended scattering timescale of $580\mu\text{s}$ but a short rise-time of $30\mu\text{s}$. Were any delayed lensed signal present, it would also have a sharp $30\mu\text{s}$ rise time which would have been detectable within the tail of the overall pulse envelope. The maximum magnification ratios (\bar{R}_f) and redshifts are similar for each burst. To calculate \bar{R}_f , the S/N (signal-to-noise ratio) of the primary peak is divided by the detection threshold (3σ). A key difference between the two is that FRB 181112 passed within 28kpc of a foreground galaxy, allowing it to probe a longer path through a galactic halo. In the following optical depth calculations these parameters are used to determine y_{\min} and y_{\max} from the equations defined in Section 2. For all following calculations, we use values for H_0 and the cosmological density parameters from the WMAP 9-yr data release ([Hinshaw et al. 2013](#)).

¹ We can also exclude circular polarization differences due to the existence of any relativistic plasma along the sightline, except at the source (where its presence would be irrelevant for the present argument). The lens mass of $10M_{\odot}$ required to explain the sub-burst time delays is significantly above the largest observed neutron star mass of $2.14M_{\odot}$ ([Cromartie et al. 2020](#)), ruling out neutron stars as potential lens candidates, and the effects of any relativistic plasma associated with them.

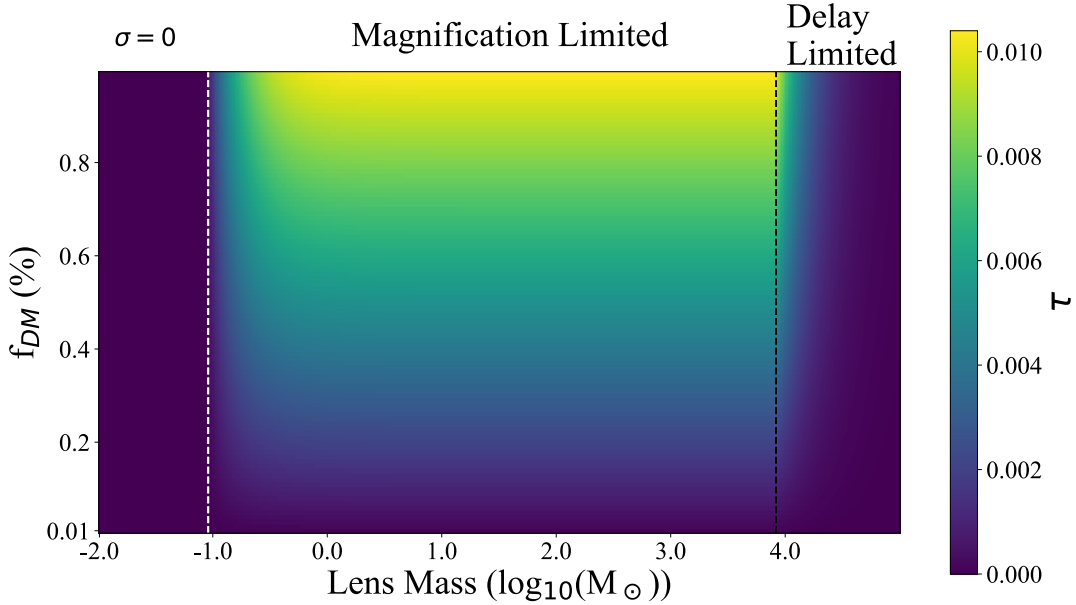


Figure 2. Optical depth to observable strong gravitational lensing by a point mass compact object of mass M_L probed by FRB 181112. For masses below the black dotted line y_{\max} is limited by the maximum magnification ratio, above y_{\max} is limited by the maximum time delay. The white dotted line marks the mass where $y_{\min}=y_{\max}$ and $\sigma = 0$. This calculation assumes a uniformly distributed population of compact objects of a single mass M_L , comprising a fraction f_{DM} of the host, Milky Way and foreground galaxies. The foreground galaxy is modelled to have a halo mass $M_{\text{halo}} = 10^{12} M_{\odot}$ (Prochaska et al. 2019) and a radius $R_{\text{halo}} = 200 \text{ kpc}$ (Shull 2014). The path length of FRB 181112 through the halo is assumed to be 400 kpc.

3.1. Halo lensing optical depth

The observable lensing cross section peaks approximately midway between the source and the observer and is minimal in both the host galaxy and the Milky way. Recently, optical followup of most arcsecond-localized FRBs, including FRB 180924, are observed not to intercept massive galaxy halos within $\sim 50 \text{ kpc}$ (Bannister et al. 2019; Chatterjee et al. 2017; Marcote et al. 2020) and are consequently of negligible value in constraining the dark matter halos of specific galaxies under our simplistic model. FRB 181112, however, passes through a foreground galaxy where the cross section to lensing is much greater, making it an ideal candidate to constrain halo lensing.

Fig. 2 displays the optical depth to observable lensing by MACHOs probed by FRB 181112. This optical depth is dominated by the contribution from the halo of the foreground galaxy. The foreground galaxy is classified as a Seyfert galaxy with an old $10^{10.69} M_{\odot}$ stellar population (Prochaska et al. 2019).

The white dotted line in Fig. 2 marks where the cross section to lensing becomes zero ($y_{\min} = y_{\max}$). Between this cutoff and a lens mass of $\sim 1 M_{\odot}$, y_{\min} and y_{\max} are comparable, and the optical depth to observing lensing depends on the mass of the lens. Above a lens mass of $\sim 1 M_{\odot}$, $y_{\max} \gg y_{\min}$ and the optical depth in the magnification-limited domain is approximately independent of mass. In the time delay-limited domain, the optical depth decreases sharply as a function of mass. We estimate that to conclude with 95% confidence that the MACHO dark matter fraction is less than 35%, we require $\sim 10^3$ FRBs that intersect a foreground galaxy similar to FRB 181112. This estimate is projected from the optical depth $\tau \approx 0.004$ probed by FRB 181112 at $f_{\text{DM}} = 0.35$. Additionally, we can conclude with 90% confidence that the total mass, in the halo of the FG galaxy of FRB 181112, contained in uniformly distributed compact objects may be no more than $2 \times 10^{14} M_{\odot}$.

3.2. Lensing by structure in the cosmic web

Fig. 3 displays the optical depth to lensing by a compact object due to any compact dark matter present throughout the cosmic web by FRB 181112 and FRB 180924, assuming that the dark matter density along their sightlines are representative of the mean cosmological dark matter density Ω_{DM} . This case shows the same trends as the halo lensing case, albeit with a much higher overall optical depth. Unlike in the halo lensing case, compact objects can be encountered anywhere in the path of an FRB. As a result, FRBs probe a much greater optical depth to lensing in this scenario. We estimate that to exclude compact dark matter fractions above 35% with 95% confidence, a comparatively

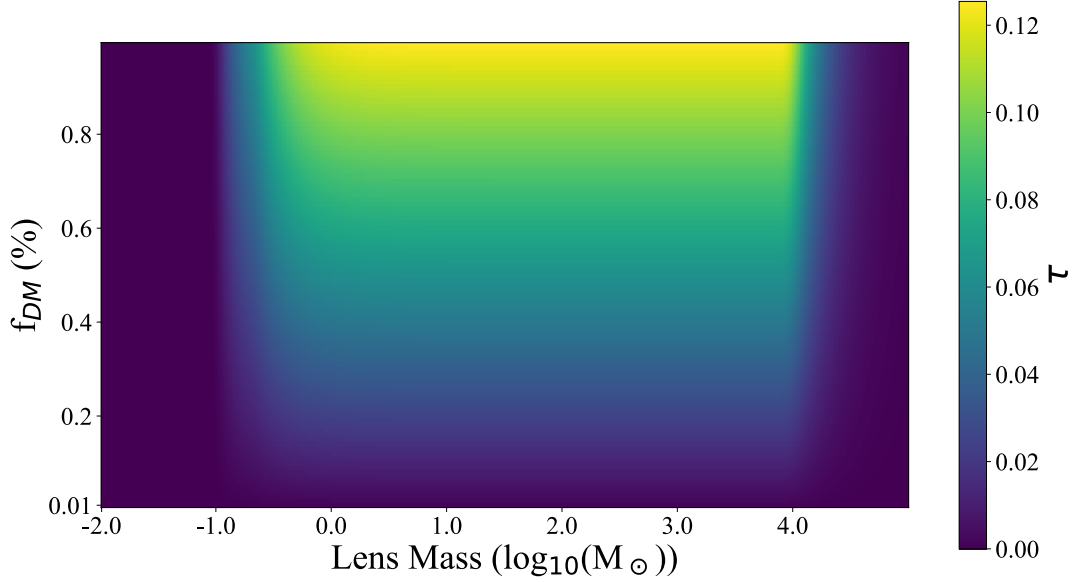


Figure 3. Optical Depth to observable strong gravitational lensing by a point mass compact object of mass M_L in the IGM probed by FRB 181112 and FRB 180924. We assume a uniform distribution of M_L mass compact objects in co-moving space comprising a fraction f_{DM} of the total dark matter of the Universe.

smaller sample of $\sim 10^2$ FRBs would be required. This estimate is projected from the average optical depth $\tau \approx 0.02$ probed by FRB 181112 or FRB 180924 at $f_{DM} = 0.35$. Under vastly different assumptions (namely an assumed FRB redshift distribution), [Laha \(2018\)](#) and [Muoz et al. \(2016\)](#) estimate that to exclude $f_{DM} \geq 1\%$ with 99% confidence, 10^4 FRBs would be required.

3.3. Gravitational Scattering

So far our treatment has been restricted to lensing by a single point mass. However, it is possible in principle that an ensemble of small masses could collectively lens an FRB signal.

We are thus motivated to examine whether gravitational scattering, caused by a cloud of substructure within a dark matter halo might occur. However, we do not yet see any evidence of scattering due to a large ensemble of low mass clumps. Within FRB 181112, we do not observe a clear exponentially decaying scattering tail, placing an upper limit to the scattering timescale $\sim 15\mu s$. The lack of this feature was interpreted as a lack of turbulent plasma along the line of sight, as discussed in [Prochaska et al. \(2019\)](#). However, it also places a constraint on the mass of lensing substructure in the intervening halo.

Clumpy dark matter could cause an achromatic scattering tail via gravitational lensing. In the limit where a large number of lenses exist within the coherence area, a statistical approach is mandated, and the characteristic delay timescale is, analogous to scattering in an inhomogeneous plasma ([Macquart 2004](#)),

$$t_{\text{scatt}} = \frac{2\pi r_F^2}{\nu r_0^2}, \quad (7)$$

where r_F is the Fresnel radius given by

$$r_F^2 = \frac{D_L D_{LS} c}{2\pi \nu D_S (1 + z_L)} \quad (8)$$

and r_0 is the length scale over which the mass density fluctuations cause the gravitational phase delay to fluctuate by one radian rms. In a simple model, where we assume a Poisson distribution of clumps (see, e.g., [Macquart 2004](#)), we have

$$r_0 = 2.2 \times 10^2 (1 + z_L)^{-1} \nu^{-1} \left(\frac{M}{1 M_\odot} \right)^{-1} \left(\frac{\Sigma}{100 \text{ clusters pc}^{-2}} \right)^{-1/2} \text{ pc}, \quad (9)$$

where Σ is the projected number density of clusters. To achieve a smooth scattering tail, the number of lenses must exceed unity within the coherence area $\sim \pi r_F^2$, to the point where the discrete contributions of individual lenses would

be indiscernible. Given that the foreground galaxy of FRB 181112 has a mass of $10^{12}M_{\odot}$ (Prochaska et al. 2019) and a radius of 200 kpc (Shull 2014), this would require that the lens masses must be much less than $\sim 5 \times 10^{-9}M_{\odot}$ for a Fresnel scale of $\sim 3\text{AU}$ (even if all the matter were contained in clumps of this size). The characteristic time delay for gravitational scattering at 1.2 GHz would therefore be much less than $\sim 6 \times 10^{-16}\text{s}$. Thus, we do not expect to observe any scattering tail associated with the lensing of a large number of small masses. Alternatively, we can state the same conclusion in terms of the number of lenses. Making the same set of assumptions about the foreground galaxy, a lens mass of $\sim 120M_{\odot}$ would be required to produce a delay with a timescale of $\sim 15\mu\text{s}$. Such a high lens mass results in fewer than one lens per coherence area, and, hence, the model is inadequate to describe the resulting temporal structure.

4. DISCUSSION

As a consequence of the greatly improved temporal resolution of FRBs 181112 and 180924 we have been able to probe to much smaller mass scales than considered in previous treatments. Longer observation of FRBs would allow greater maximum temporal separations to be observed, extending the mass independent regime of any constraints to higher masses. Improvements to sensitivity will boost S/N and increase y_{max} in the magnification-limited regime. A larger y_{max} yields a larger cross section and consequently a greater observable lensing optical depth, thus providing a more sensitive probe to small scale structure.

FRBs captured at high time resolution represent an opportunity to explore fine structure of galaxy halos and clusters on unprecedented scales. We have focused here on the potential for FRBs to detect compact objects and derived simple constraints on non-baryonic dark matter models. The favoured ΛCDM cosmology is well known for its success describing the large scale structure of our Universe, but it faces a number of challenges on length scales below 1 Mpc (Bullock & Boylan-Kolchin 2017). To meet these challenges, the substructure of dark halos must be understood, and, as shown, high time resolution FRBs provide us with the means to do so.

To exclude lensing with 95% confidence, a cumulative optical depth of 3.0 is required. From Figures 2 and 3, we estimate the optical depth probed by an FRB similar to those considered here at a range of compact dark matter fractions. The cumulative optical depth probed by a set of FRBs is simply the summation of their individual optical depths as per eq. 4. Hence, we can predict the number of FRBs that would be required to make a desired constraint. The number required varies with f_{DM} , the desired confidence level and the assumed distribution (e.g. in halos or distributed throughout the cosmic web). The cumulative optical depth required is non-linear with the desired level of confidence, and, hence, a lesser constraint of 80-90% would require a sample of 54-77% the size. Conversely, the cumulative optical depth required is linear with the compact dark matter fraction, i.e. to exclude the compact dark matter fraction with the same confidence to below $0.5f_{\text{DM}}$ requires a sample twice the size.

In summary, recent FRBs detections, made at high time resolution, have revealed the potential of FRBs to probe dark matter within our Universe. The fact that FRBs have narrower temporal structure than previously assumed in gravitational lensing studies, allows searches for smaller lens masses than previously considered. The probability of observing halo lensing, in an FRB similar to 181112, is ~ 0.004 (assuming $f_{\text{DM}} \leq 0.35$). To exclude $f_{\text{DM}} \geq 0.35$, in galaxy halos, would require a sample of $\sim 10^3$ FRBs like FRB 181112. The probability of observing lensing anywhere along the sightline, in an FRB similar to FRB 181112 or FRB 180924, is ~ 0.02 (assuming $f_{\text{DM}} \leq 0.35$). This is a lower limit, in the sense that a large fraction of FRBs have dispersion measures that place them at higher redshifts than these two bursts and it ignores the possibility that the sample of already detected bursts favours lensed events through magnification bias. Thus, it is possible that a significant number of the sample of > 100 FRBs known to date have been lensed, although the lower time resolution and lower S/N of a large fraction of these previous detections would substantially hinder the discoverability of any lensing signal. To exclude $f_{\text{DM}} \geq 0.35$, in the IGM, would require detection of $\sim 10^2$ FRBs similar to FRB 181112 or FRB 180924. Finally, we conclude that the volume filling factor of dark matter in the foreground galaxy of FRB 181112 is likely insufficient to contribute to the temporal scatter-broadening of FRBs on nanosecond to microsecond timescales.

J.P.M. and R.M.S. acknowledge Australian Research Council (ARC) Grant DP180100857. R.M.S. is the recipient of ARC Future Fellowship FT190100155.

REFERENCES

- Alcock, C., Allsman, R. A., Alves, D., et al. 1997, *The Astrophysical Journal*, 479, 119.
<https://iopscience.iop.org/article/10.1086/303851/meta>
- Atri, P., Miller-Jones, J. C. A., Bahramian, A., et al. 2019, arXiv:1908.07199 [astro-ph], arXiv: 1908.07199.
<http://arxiv.org/abs/1908.07199>
- Bannister, K. W., Deller, A. T., Phillips, C., et al. 2019, *Science*, 365, 565.
<https://science.sciencemag.org/content/365/6453/565>
- Bennett, C. L., Larson, D., Weiland, J. L., et al. 2013, *The Astrophysical Journal Supplement Series*, 208, 20.
<https://ui.adsabs.harvard.edu/abs/2013ApJS..208...20B/abstract>
- Bertone, G., Hooper, D., & Silk, J. 2005, *Physics Reports*, 405, 279, arXiv: hep-ph/0404175.
<http://arxiv.org/abs/hep-ph/0404175>
- Bhandari, S., Keane, E. F., Barr, E. D., et al. 2018, *Monthly Notices of the Royal Astronomical Society*, 475, 1427. <https://academic.oup.com/mnras/article/475/2/1427/4668427>
- Bird, S., Cholis, I., Muoz, J. B., et al. 2016, *Physical Review Letters*, 116, 201301. <https://link.aps.org/doi/10.1103/PhysRevLett.116.201301>
- Brandt, T. D. 2016, *The Astrophysical Journal*, 824, L31.
<https://doi.org/10.3847/2F2041-8205%2F824%2F2%2F131>
- Bullock, J. S., & Boylan-Kolchin, M. 2017, *Annual Review of Astronomy and Astrophysics*, 55, 343, arXiv: 1707.04256. <http://arxiv.org/abs/1707.04256>
- Chatterjee, S., Law, C. J., Wharton, R. S., et al. 2017, *Nature*, 541, 58.
<https://www.nature.com/articles/nature20797>
- Cho, H., Macquart, J.-P., Shannon, R. M., et al. 2020, *ApJL*
- Clesse, S., & Garca-Bellido, J. 2017, *Physics of the Dark Universe*, 15, 142, arXiv: 1603.05234.
<http://arxiv.org/abs/1603.05234>
- Coward, D., Howell, E., Branchesi, M., et al. 2013, *Monthly Notices of the Royal Astronomical Society*, 432, 2141, arXiv: 1210.2488. <http://arxiv.org/abs/1210.2488>
- Cromartie, H. T., Fonseca, E., Ransom, S. M., et al. 2020, *Nature Astronomy*, 4, 72, arXiv: 1904.06759.
<http://arxiv.org/abs/1904.06759>
- Farah, W. 2020, private communication, ,
- Hinshaw, G., Larson, D., Komatsu, E., et al. 2013, *The Astrophysical Journal Supplement Series*, 208, 19, arXiv: 1212.5226. <http://arxiv.org/abs/1212.5226>
- Ji, L., Kovetz, E. D., & Kamionkowski, M. 2018, *Physical Review D*, 98, 123523, arXiv: 1809.09627.
<http://arxiv.org/abs/1809.09627>
- Jow, D. L., Foreman, S., Pen, U.-L., & Zhu, W. 2020, arXiv:2002.01570 [astro-ph], arXiv: 2002.01570.
<http://arxiv.org/abs/2002.01570>
- Laha, R. 2018, arXiv:1812.11810 [astro-ph, physics:hep-ex, physics:hep-ph], arXiv: 1812.11810.
<http://arxiv.org/abs/1812.11810>
- LIGO Scientific Collaboration and Virgo Collaboration, Abbott, B., Abbott, R., et al. 2019, *Physical Review X*, 9, 031040.
<https://link.aps.org/doi/10.1103/PhysRevX.9.031040>
- Macquart, J.-P. 2004, *Astronomy & Astrophysics*, 422, 761, arXiv: astro-ph/0402661.
<http://arxiv.org/abs/astro-ph/0402661>
- Marcote, B., Nimmo, K., Hessels, J. W. T., et al. 2020, *Nature*, 577, 190, arXiv: 2001.02222.
<http://arxiv.org/abs/2001.02222>
- Muoz, J. B., Kovetz, E. D., Dai, L., & Kamionkowski, M. 2016, *Physical Review Letters*, 117, 091301, arXiv: 1605.00008. <http://arxiv.org/abs/1605.00008>
- Prochaska, J. X., Macquart, J.-P., McQuinn, M., et al. 2019, arXiv:1909.11681 [astro-ph], arXiv: 1909.11681.
<http://arxiv.org/abs/1909.11681>
- Quinn, D. P., Wilkinson, M. I., Irwin, M. J., et al. 2009, *Monthly Notices of the Royal Astronomical Society: Letters*, 396, L11, arXiv: 0903.1644.
<http://arxiv.org/abs/0903.1644>
- Sasaki, M., Suyama, T., Tanaka, T., & Yokoyama, S. 2016, *Physical Review Letters*, 117, 061101, arXiv: 1603.08338.
<http://arxiv.org/abs/1603.08338>
- Shull, J. M. 2014, *The Astrophysical Journal*, 784, 142, arXiv: 1401.5799. <http://arxiv.org/abs/1401.5799>
- Tisserand, P., Guillou, L. L., Afonso, C., et al. 2007, *Astronomy & Astrophysics*, 469, 387, arXiv: astro-ph/0607207.
<http://arxiv.org/abs/astro-ph/0607207>
- Wong, K. C., Suyu, S. H., Chen, G. C.-F., et al. 2019, arXiv:1907.04869 [astro-ph], arXiv: 1907.04869.
<http://arxiv.org/abs/1907.04869>
- Wyzykowski, L., Skowron, J., Kozłowski, S., et al. 2011, *Monthly Notices of the Royal Astronomical Society*, 416, 2949, arXiv: 1106.2925. <http://arxiv.org/abs/1106.2925>
- Zumalacarregui, M., & Seljak, U. 2018, arXiv:1712.02240 [astro-ph, physics:gr-qc, physics:hep-ph, physics:hep-th], doi:10.1103/PhysRevLett.121.141101, arXiv: 1712.02240.
<http://arxiv.org/abs/1712.02240>